

Development of Ultra-Low NO_x Combustor Technology for Next Generation Supersonic Transport Engines in ESPR Project

Shigeru Hayashi¹, Hideshi Yamada¹, Kazuo Shimodaira¹, Seiji Yoshida¹,
Takeo Oda², Hiroyuki Ninomiya², and Bryn Jones³

¹Japan Aerospace Exploration Agency
7-44-1 Jindaijihigashi, Chofu, Tokyo, JAPAN
Phone: +81-422-40-3411, Fax: +81-422-40-3445, E-mail: hayashi.shigeru@jaxa.jp
²Kawasaki Heavy Industries Ltd
Kawasaki, Akashi, Hyogo, JAPAN
³Rolls-Royce plc.

ABSTRACT

Ultra-low NO_x combustor technology is being developed for aero engines of the next generation supersonic transport in the ESPR program. The emissions of a single sector staged combustor with a main burner of lean premixed and prevaporized type and a pilot were evaluated at major operating conditions including cruise. Neither flashback nor autoignition occurred at either take-off or cruise conditions even when the mixture velocity was halved. The NO_x emissions are encouraging in that an EINO_x of 3.8 g/kg-fuel has been achieved at conditions simulating a supersonic passenger aircraft engine at Mach 2.2 cruise.

INTRODUCTION

This research conducted since 1998 forms part of the Research and Development of Environmentally Compatible Propulsion System for Next-Generation Supersonic Transport (ESPR) project [1], an international collaboration sponsored by the Ministry of Economy, Trade and Industries. The targeted engine is a turbojet with a rated thrust of 350 kN for a 300 passenger supersonic transport propelled by four engines that can cruise at flight Mach numbers up to 2.2. Development of ultra-low NO_x combustor technology is one of the most important objectives of the program as in overseas SST propulsion technology development programs [2] since the NO_x in the exhaust from supersonic transports cruising in the lower stratosphere can deplete ozone concentration.

A two-thirds flow scale model of the target engine had already been manufactured as the turbojet part of the experimental combined cycle engine in the HYPR project that preceded the ESPR project. This effort was directed towards the application of lean premixed and prevaporized (LPP) combustion to this existing experimental turbojet engine. The combustor inlet and outlet conditions at major operation modes of this engine are listed in Table 1. The NO_x reduction target in the project is to achieve no more than 5 grams of NO₂ per kilogram of fuel burned at simulated cruise conditions. The total emissions of CO, HC and NO_x during the ICAO LTO cycle are to meet the latest ICAO emissions standards with a 50% margin.

The combustor for the experimental ESPR turbojet engine is of a stepped dome configuration with the main combustion zone in the outer dome and the pilot combustion zone in the inner dome. The main combustion zone is axially shifted downstream with respect to the pilot combustion zone. Most of the dimensions of the

combustor such as dome height, total combustor liner length and inner and outer diameters of the combustor exit passage are restricted so that the combustor can be installed in the existing ESPR engine with minimum modification.

EXPERIMENTAL COMBUSTOR

Preliminary tests have been conducted on several main and pilot burners to evaluate their potential for ultra-low NO_x emissions. A configuration of a single converging tube with multiple swirlers and prefilming air-blast fuel atomizers has been selected for the LPP main burner due to its robustness and resistance to auto-ignition and flashback. A hybrid burner consisting of concentric air-blast atomizers was selected for the pilot burner.

Figure 1 shows a schematic drawing of the single sector combustor test unit and a photo of the LPP pre-mixer. The sidewalls of the single sector combustor test unit were made of thermal insulating ceramic and the inner and outer combustion liner metal walls were cooled by angled effusion with thermal barrier coating. It was estimated that about 18% of the total airflow was used for cooling the liner walls and dome heat shield.

The pre-mixer tube was a straight converging circular tube of 100 mm in total length, tapering from 85 to 58 mm in diameter from inlet to outlet. The axial distance from the prefilming lip of the air-blast fuel atomizer to the pre-mixer outlet was 85 mm. Residence times are shorter than one millisecond. It is noted that the auto ignition delay at the most severe conditions of the engine is estimated to be around 2 ms.

The pilot burner has an annular passage and a cylindrical passage. The fuel flow rates to these two passages were independently modulated to optimize NO_x emissions at high thrust CO and HC emissions at low thrust. In the outer atomizer, fuel is supplied to the cylindrical prefilmer surface to produce a thin sheet in the outer passage before being atomized by swirling inner and outer air jets at the lip. The fuel to the inner atomizer is injected through radial holes on the cylinder wall and the fuel jets bridge the air stream to impinge the second prefilmer. The resulting fuel sheet is atomized at the lip by interaction between the inner and outer swirling air flows and the fuel sheet.

The outer and inner combustor liner walls, made of curved panels with flanges, are bolted to the sidewalls. The radii of the inner and outer liner walls are 220 and 435 mm at dome and 268 and 341 mm at the exit.

EXPEERIMENTAL PROCEDURE

Tests were conducted using the AP-7 High-Temperature, High-Pressure combustion test rig at the National Aerospace

Laboratory. Kerosine was used as the fuel. Exhaust gas was sampled by a water-cooled gas-sampling rake consisting of four tubes arranged circumferentially placed just downstream of the combustor exit. Each tube had eight holes of 2-mm in diameter radially equi-spaced. Gaseous emissions were evaluated over a range of equivalence ratios at combustor inlet pressures and temperatures simulating the major engine operating modes listed in Table 1.

FLOW MEASUREMENTS

To understand the effectiveness of counter rotational swirl in preventing recirculation or very slow axial flow in the region around the axis of the premixer tube, flow measurements downstream of the premixer were conducted by particle image velocimetry. A model representing the outer volume of the single sector combustor was fabricated. Optical grade flat glass plates were fitted to both sides and top of the flow model for optical access. The measurements were conducted under isothermal conditions of 400 K inlet air temperature and atmospheric pressure. The average velocity of air at the premixer exit, 63 mm in inner diameter, was limited by the flow meter to 40 m/s, less than half the design value. The laser sheet was in x-y planes, $z = -10, 0, 10, 20$ mm. Figure 2 shows the velocity field on plane $z = 0$. Figure 3 shows contours of axial velocity (x-direction) and v-component velocity on the y-z plane at $x = 18$ mm. These results clearly show that neither a recirculation nor low velocity zone is formed at the exit of the premixer and that the circumferential velocity is very low in the center region while strong in the annular zone at 0.7 non-dimensional radius. The counter rotating flows from the inner two swirlers merge, cancelling the swirl and preventing recirculation along the center axis. This type of flow field is effective in preventing flashback into the premixing tube while maintaining effective mixing of fuel and air. Neither flashback nor auto-ignition in the premixer tube has been experienced at simulated take-off and cruise conditions even when the air velocity was intentionally reduced as low as a half of the design value.

EMISSIONS RESULTS

Figure 4 shows the emission indices for NO_x and combustion efficiency as a function of overall air-fuel ratio, calculated based on gas analysis, at combustor cruise conditions, 920 K inlet air temperature and 11 bar pressure. The air split between the main and pilot combustion zones, calculated from flow coefficient measurements, is estimated to be 70:30. Some preliminary test data showed that while maintaining total fuel flow to the main burner, NO_x increased with increasing fuel proportion to the center injector of the main burner even when the amount was only a few percent of the total fuel flow. The fairly flat radial profiles of air-fuel ratio measured at the premixer exit without fuel injection from the center injector suggest that the center injector is unnecessary. Deleting center fuel injection is welcome since it simplifies both the injector and fuel system. Therefore, most of the data were obtained for fuel injection from the outer atomizer alone.

The distribution of fuel among the main burner, and outer and inner atomizers of the pilot burner was modulated to find an optimum for NO_x emissions. The optimal fuel split between main burner and the outer and inner atomizers of the pilot burner was found to be around 70:30:0. As with the main burner, a small amount of fuel injected from the pilot inner atomizer resulted in a noticeable increase in NO_x emissions.

The EINO_x increases steeply with decreasing air-fuel ratio. A decrease in air-fuel ratio from 35 to 27 resulted in a greater than eight times increase in NO_x. Although the lowest EINO_x was obtained without fuel injection from the center atomizer of the pilot burner, some fuel is necessary to secure flame stability at low power. At the designed air-fuel ratio of 31, the EINO_x was 3.8 g/kg-fuel. The NO_x emission target in the full annular combustor tests, scheduled this winter, is 5 g/kg-fuel. Thus, this result is very

encouraging.

The carbon monoxide and unburned hydrocarbon emissions at cruise are shown in Fig. 5. These emissions are very low and combustion is complete. The major reason are enhanced evaporation of the fuel spray in the premixer due to high inlet air temperature and enhanced oxidation reaction of unburned species due to high gas temperatures in the combustion chamber.

The EINO_x, together with combustion efficiency, at the inlet air temperature and pressure simulating take-off are plotted in Fig. 6 as a function of overall air-fuel ratio. The combustion efficiency remains very close to 100% at the target engine design air-fuel ratio of 33.3 though it begins to decrease on the leaner side. A small amount of fuel injected into the inner atomizer of the pilot burner resulted in an appreciable increase in NO_x emissions, showing that the mixture from the inner air-blast atomizer is closer to the stoichiometric air-fuel ratio than the mixture from the outer atomizer. The EINO_x at the air-fuel ratio of 33.3 is much less than unity. The EINO_x of the targeted engine is smaller at take off than at cruise, which is specific to aero engines for an SST. The opposite is true for subsonic engines.

In the target engine cycle, both combustor inlet air and outlet gas temperatures are higher at cruise than at take off while the pressure is about 1.7 times larger at take off than at cruise. The EINO_x from diffusion flame combustion increases with pressure, being generally proportional to the 0.4-0.6 power of pressure. On the other hand, the NO_x formation in lean premixed combustion is less sensitive to or almost independent of pressure. Thus, efforts are being directed to controlling NO_x at cruise in the development of ultra-low NO_x combustor technology for the SST. The concentration of carbon monoxide and hydrocarbons in the exhaust gas are shown in Fig. 7.

The target engine design air-fuel ratio at approach is 56. The combustion efficiency data at simulated take-off conditions, plotted in Fig. 6, clearly showed that, if fuel is distributed between main and pilot burners at a ratio of 70:30 at simulated approach conditions, combustion would be significantly incomplete. The NO_x emissions would be significantly high if only the pilot burner is fueled. The conflict between efficiency and NO_x at approach may perhaps be resolved by operating with all pilot burners and only a proportion of the main burners fuelled. It is of course impossible to investigate this option with a single sector rig. Thus, in the present test, emissions were evaluated at air-fuel ratios greater than the design value with the main burner unfueled and the pilot burner fueled.

The measured EINO_x and combustion efficiency are plotted in Fig. 8 as a function of overall air-fuel ratio. Figure 9 shows the CO and HC emissions at these conditions. The optimum overall air-fuel ratio for the pilot burner fueling is around 85, as compared with the design air-fuel ratio of 66. It seems likely that one in six of the main injectors would have to be lit, to optimize the fuel distribution.

Another consideration at approach is the radial temperature distribution into the turbine. If all fuel is fed through one bank of injectors only, overheating at blade root or tip is probable. The possible impact of circumferential staging on blade vibration and turbine efficiency is unknown, although the method has been used successfully in some production engines such as the CFM56.

The estimated total emissions of CO and HC during the ICAO LTO cycle would marginally meet the standard with fuel split between optimal numbers of main and pilot burners at each thrust. Therefore, optimization of air split between the main and pilot burners and fuel staging among the main burners should be the most important issue in the next phase of combustion development.

Figure 10 shows a correlation between EINO_x with calculated adiabatic gas temperatures from combustor exit air-fuel ratio. The plots for each set of conditions are close to a straight line. The slopes of the lines for the data sets at simulating cruise and take-off conditions are the same, being steeper than that for approach.

In the HYPR project, single flame tube tests of LPP premixers

were conducted at similar operating conditions [3]. The NOx emissions are shown in the figure for comparison. The dotted line shows the data for a scaled LPP burner and the broken line those for a burner of a realistic size. The NOx level was higher with the large size pre-mixer. This is because homogeneous mixtures can be more easily prepared in a smaller diameter pre-mixer. The slopes of the lines for the previous and present experiments are of similar magnitude.

An Arrhenius plot of the exhaust NOx concentrations is shown in Fig. 11, where T_b is the adiabatic combustor exit gas temperature. At cruise and take off the data plots for EINOx are on a single straight line for a given fuel splits between the center and outer atomizers of the pilot burner. This shows that the NOx formation is independent of pressure.

The resulting equations for correlating $\log [NO_x]$ with $-1/T$ for the three lines in the figure are as follows:

$$NO_x = 1.69 \times 10^{10} \exp(-401 \times 10^3 / RT)$$

$$1.82 \times 10^{10} \exp(-320 \times 10^3 / RT)$$

$$0.457 \times 10^{10} \exp(-305 \times 10^3 / RT)$$

The slope for EINOx with fuel injection to the pilot center atomizer is smaller than that for the counter part. The slope for EINOx at simulated approach is the same with that at take off and cruise, where fuel was injected into the center atomizer of the pilot burner as well.

The values of the overall activation energy are close to or larger than the value of 314 kJ/mol for the reaction $N_2 + O = NO + N$, the rate controlling reaction in the Zeldovich mechanism for thermal NO formation. The good agreement obtained between the present values and previously reported values for NOx from combustion of homogeneously premixed gas mixtures suggest that homogeneous mixing was achieved in the pre-mixer.

In the present tests, almost fully vaporized atomized fuel seems

to have mixed with air to produce a fairly uniform mixture in the pre-mixer at all conditions tested. Fuel evaporation seems almost complete at the higher inlet air temperatures at takeoff and cruise conditions.

CONCLUSIONS

1. Good margin for flash back and auto-ignition were demonstrated at the most severe engine operating conditions for the next generation super sonic transport.
2. Combination of counter rotational swirl around the axis is found to be very effective in preventing recirculation or low-velocity regions, which would favor flash back or auto-ignition.
3. NOx emissions lower than 5g/kg-fuel were achieved at the simulated engine operating conditions at cruise
4. Optimum fuel staging and split is critical at low thrust for achieving high combustion efficiency while maintaining acceptable NOx emissions.

REFERENCES

- [1] Yamaguchi, Y., Miyazawa, K., and Fujitsuna, Y., Overview of "Research and Development of Environmentally Compatible Propulsion System for Next-Generation Supersonic Transport (ESPR Project)", 15th ISABE, Paper No. 2001-1180, 2001.
- [2] Shaw R.J., Koops L.W. and Hines R., Progress Toward Meeting the Propulsion Technology Challenges for the High Speed Civil Transport, 14th ISABE Paper No. 99-7005, 1999.
- [3] Jones, B., Research and Development of a Low NOx Combustor for HYPR Turbojet Engine-Kerosene Fueled, Third International Symposium on Japanese National Project for Super/Hyper-sonic Transport Propulsion System, pp.137-143, 1999.

Table.1. Combustor operating conditions at major engine thrust settings.

Operating conditions	Idle	Approach	Climb	Take off	Cruise
Air temperature, K	466	618	737	790	915
Pressure, MPa	0.38	1.02	1.27	1.88	1.13
Air-fuel ratio	96.8	55.9	35.5	33.3	31.0
Exit temperature, K	865	1253	1664	1760	1924

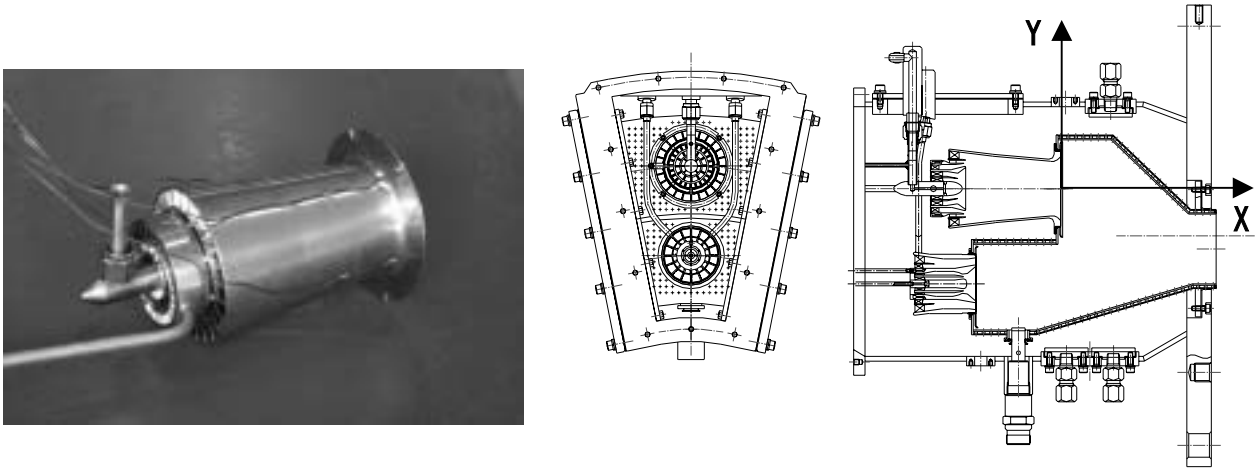


FIG.1. Schematic drawing of single sector combustor with a main burner in outer dome and a pilot burner in inner dome (right) and photo of LPP premixer

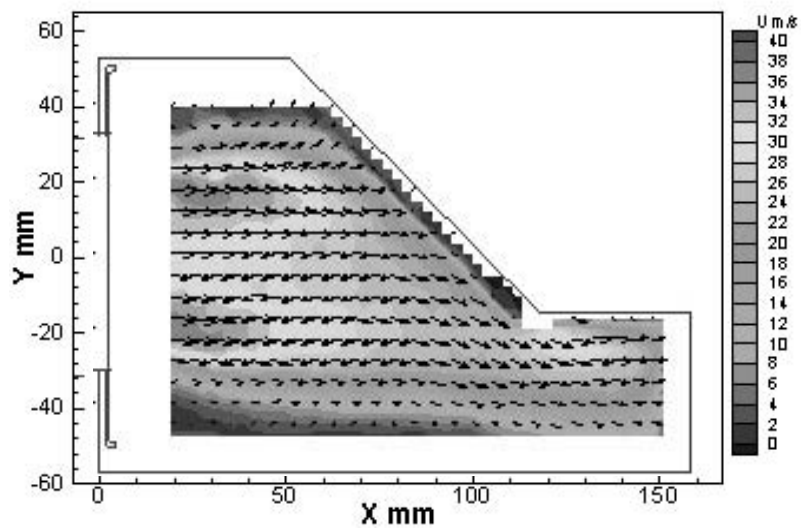


FIG.2. Axial velocity field in $z = 0$ plane measured by PIV

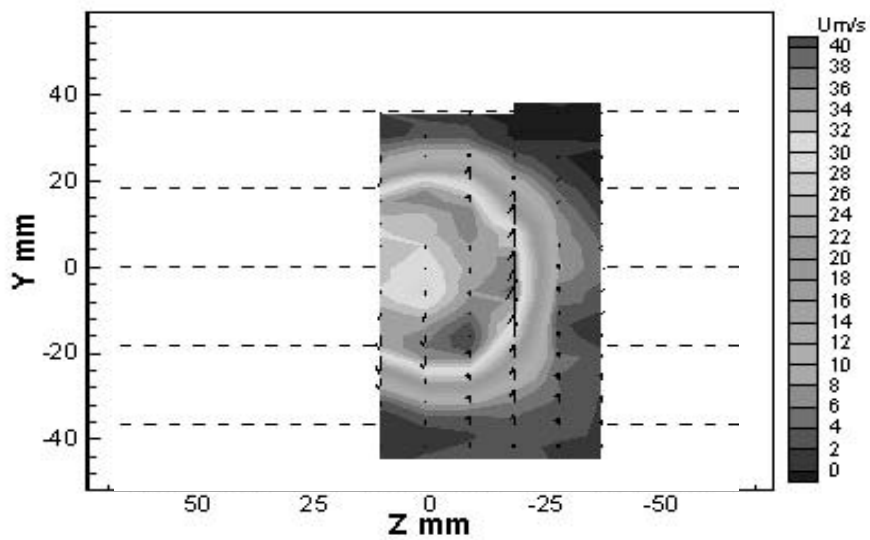


FIG.3. Axial velocity contour and v-component of velocity at $x = 18$ mm measure by PIV.

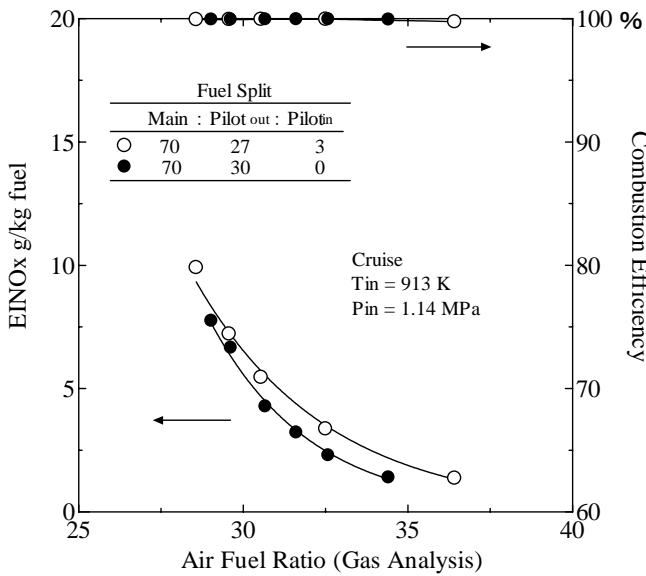


FIG.4. Effects of overall equivalence ratio on NOx emissions and combustion efficiency at conditions simulating cruise for different fuel splits.

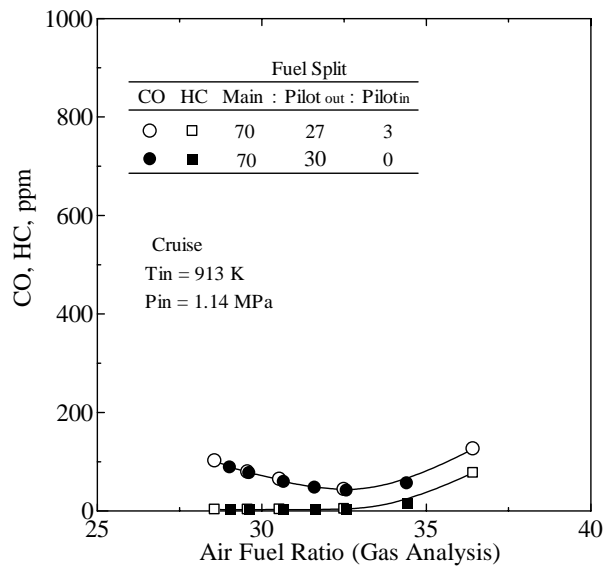


FIG.5. Effects of overall equivalence ratio on concentrations of CO and HC in exhaust at conditions simulating cruise for different fuel splits.

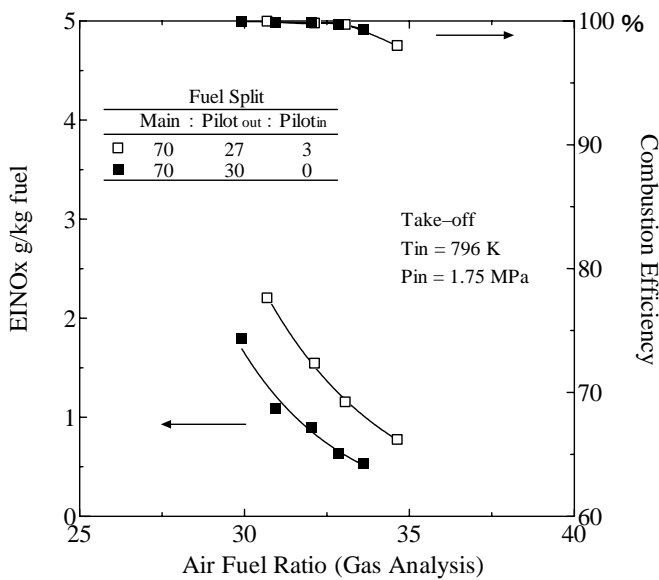


FIG.6. Effects of overall equivalence ratio on NOx emissions and combustion efficiency at conditions simulating take-off for different fuel splits.

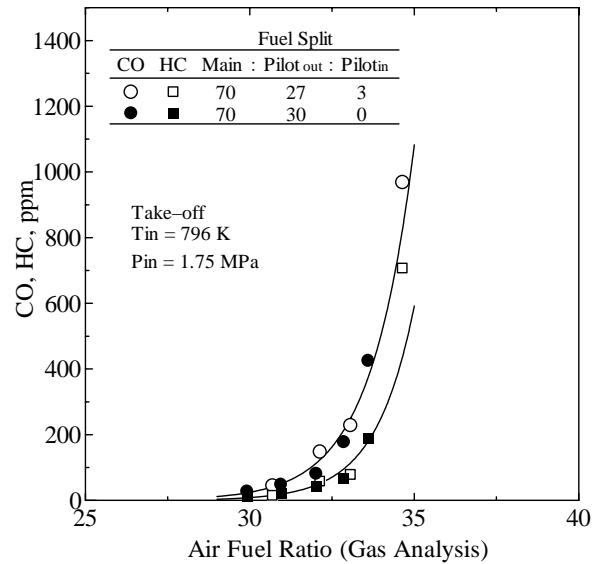


FIG.7. Effects of overall equivalence ratio on concentrations of CO and HC in exhaust at conditions simulating take-off for different fuel splits

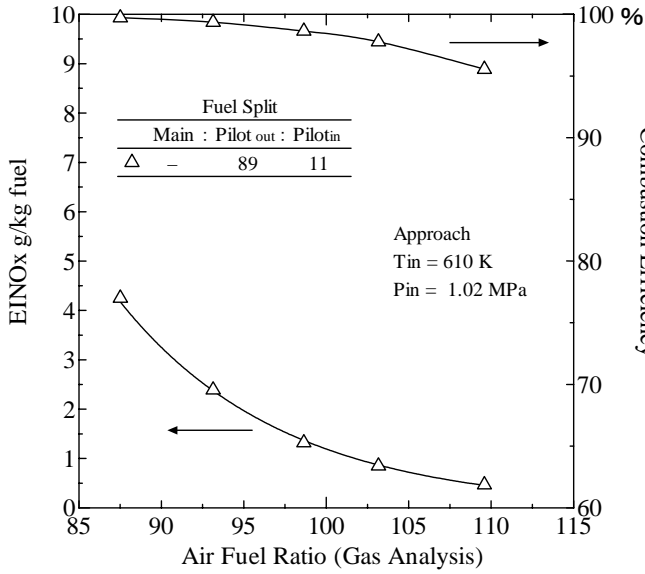


FIG.8. Effects of overall equivalence ratio on NOx emissions and combustion efficiency at conditions simulating approach.

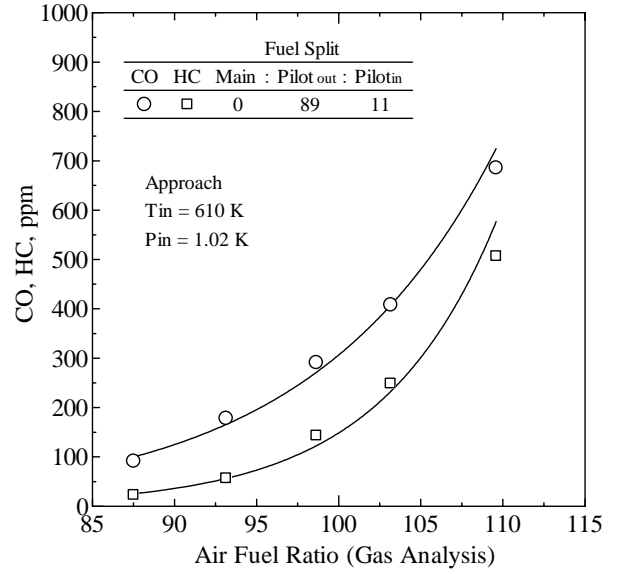


FIG.9. Effects of overall equivalence ratio on concentrations of CO and HC in exhaust at conditions simulating approach.

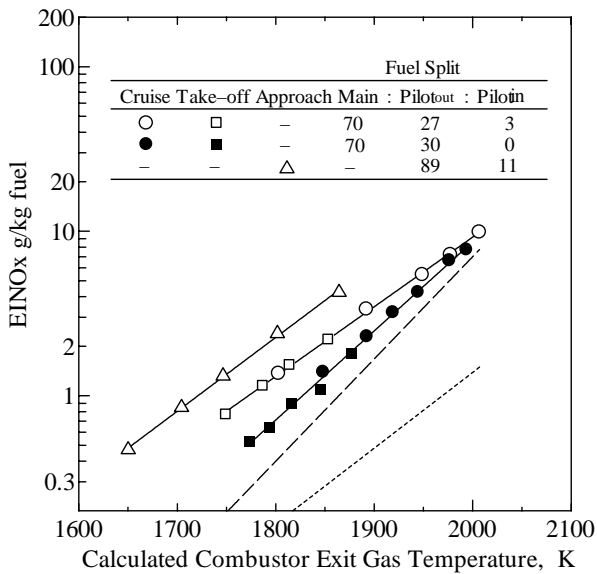


FIG.10. Correlation of EINOx at different conditions with combustor exit gas temperature. Dotted and broken lines show previous data for LPP burners in flame tube emissions tests (Ref. [3]).

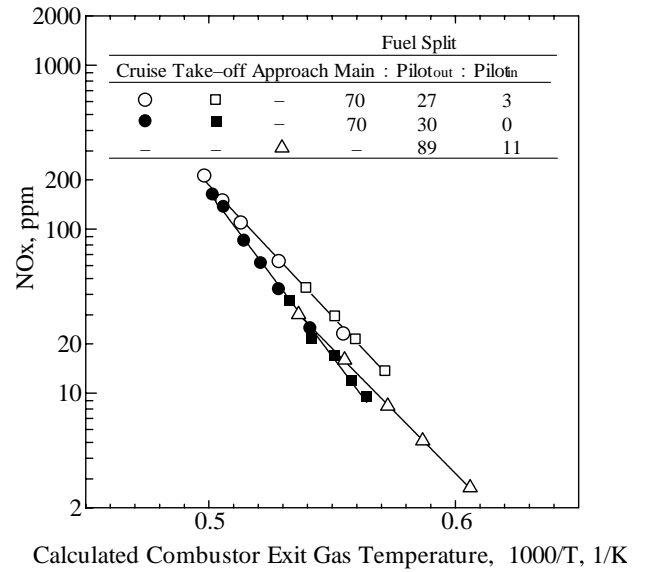


FIG.11. Arrhenius plots of NOx in exhaust gas.